

## Instability of Taylor-Sedov Blast Waves Propagating through a Uniform Gas

J. Grun, J. Stamper,<sup>(a)</sup> C. Manka, J. Resnick,<sup>(b)</sup> R. Burris,<sup>(c)</sup> J. Crawford,<sup>(d)</sup> and B. H. Ripin  
*Space Plasma Branch, Plasma Physics Division, Naval Research Laboratory, Washington, D.C. 20375-5000*  
 (Received 10 January 1991)

We present the first measurements of an instability in Taylor-Sedov blast waves propagating through a uniform gas. The instability occurred in a gas whose adiabatic index was low. Amplitude perturbations grew as a power of time. Our observations are compared to theory.

PACS numbers: 47.40.Nm, 28.70.+y, 47.20.-k, 52.35.Tc

Blast-wave instability may contribute to the structuring observed in supernovae and play a role in the formation of stars and galaxies.<sup>1</sup> Unfortunately, knowledge of blast-wave instabilities is based almost entirely on theoretical considerations, and these have been accompanied by considerable controversy.<sup>2-4</sup> Unstable blast waves had not been observed experimentally, leading some to conclude that blast waves must be stable.<sup>3</sup>

We present the first measurements of an instability in Taylor-Sedov blast waves<sup>5</sup> propagating through a uniform gas. The instability occurred in an ambient gas whose adiabatic index  $\gamma$  was a low  $1.06 \pm 0.02$ . Perturbations grew as a power of time. Our observations are compared to a theory described in papers by Vishniac and Ryu.<sup>4</sup>

Blast waves, in our experiment, are produced by the expansion of ablation plasma from the surface of laser-irradiated foils into an ambient gas (Fig. 1). A 6- $\mu\text{m}$ -thick polystyrene foil is placed in a chamber which is first evacuated and then filled to 5-torr pressure of nitrogen or xenon gas. The foil surface is heated<sup>6</sup> to about 800 eV with a 200-J, 1.054- $\mu\text{m}$ , 5-ns pulse from the Pharos III Nd-glass laser, which is focused to a 3-TW/cm<sup>2</sup>, 880- $\mu\text{m}$ -diam spot. Ablation plasma from the hot foil surface propagates supersonically into the background gas<sup>7</sup> at about 700 km/s and, much like the products of a chemical explosion, forms a blast wave. (Simultaneously, the background gas is photoionized by radiation from the vicinity of the laser's focal point.)

We have verified through extensive experimentation that this laser-ablation method forms classical Taylor-Sedov blast waves when the interaction between the ablation plasma and the gas is collisional, and when the mass of the swept-up ambient gas is greater than the mass of the ablation plasma.<sup>8</sup> For nitrogen, collisional coupling occurs at gas pressures exceeding 0.5 torr.

Blast-front structure is photographed using the well-known dark-field imaging method, which is sensitive to the square of fluctuations in the index of refraction. In our implementation, a 0.53- $\mu\text{m}$ , < 1-ns-duration, 5-cm-diam, few-mJ laser probe illuminates the blast wave side-on. Electron-density gradients within the blast wave deflect a part of the probe while the remainder passes through undisturbed. The probe beam emerging from the blast-wave region is then relayed onto a film surface with a telescope. A stop placed at a focal point inside the telescope blocks the undisturbed component of the probe light but passes the deflected part, thereby forming an image in which fluctuations in the index of refraction (and hence electron density) appear as bright features on a dark background.

In addition, visible emission from the blast front is photographed with a very fast (120-ps to 5-ns gate time), four-frame, microchannel-plate intensifier camera. This, together with the dark-field image, provides five photographs per shot of the blast wave at different times in its evolution. The dynamics of the blast wave are reconstructed by combining the results of dark-field and emission photographs taken at different times on individual and multiple shots. Also, the spectrum of light emitted by the ambient gas before and after the passage of the blast wave is measured with temporal and spatial resolution. To do this, we image a 3-mm-diam spot in front of the foil onto the slit of a spectrometer and record the resulting spectrum with a streak camera.

We find that Taylor-Sedov blast waves formed in nitrogen gas are always stable and smooth—like the example in Fig. 2(a). In startling contrast [Fig. 2(b)], the surface of the blast fronts launched into an ambient xenon gas is wrinkled like a dried prune. This wrinkling is quantified by tracing and then Fourier transforming<sup>9</sup> the outer edge of the front, which is equivalent to looking at the projection onto a plane of the edge of an unstable

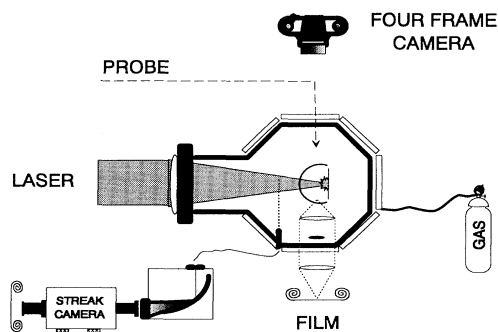


FIG. 1. Experimental setup.

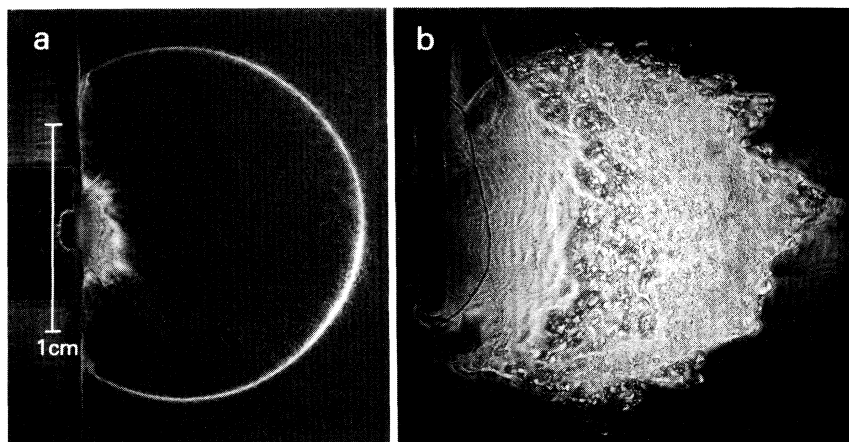


FIG. 2. Dark-field shadowgraph of (a) a stable blast wave in nitrogen gas, and (b) an unstable blast wave in xenon gas (at 243 ns).

sphere. The results are presented as  $A_t(k)/R$  vs  $\log_{10}(kR)$ , where  $A_t(k)$  is the full amplitude of the mode with wave number  $k$  at time  $t$ , and  $R$  is the average radius of the blast-front boundary.

The blast-wave trajectory in xenon and the evolution of instability amplitude  $A_t(k)/R$  are shown in Fig. 3. From 6 to 18 ns the front moves at a constant speed corresponding to the velocity of the ablation plasma, a blast wave not yet having formed. The front is slightly structured, but these nonuniformities do not grow. By 25 ns a blast wave propagating with the  $t^{2/5}$  Taylor-Sedov dependence has formed. Now the surface becomes significantly more wrinkled and spikelike protuberances shoot ahead of the front:  $A_t(k)/R$  increases as a power of time until 300 ns. It is noted that the blast wave does not fall apart or otherwise dissipate, but propagates as a shocklike, albeit structured, front. As the protuberances get larger they become increasingly more difficult to observe. By 400 ns they are not seen at all and the blast wave takes on the appearance of a slightly structured but basically stable shock.

A power law of the form  $A_t(k)/R \cong t^{S(kR)}$  was fitted to the  $A_t(k)/R$ -vs-time data during the period of growth, with the results shown in Fig. 3(c). We find clear growth for modes satisfying  $0.7 < \ln(kR) < 2$ . Maximum growth occurs at  $\ln(kR)=1$ , where  $S=1.6$ , and minimum growth, with  $S=0.3$ , occurs at  $\ln(kR)=2$ . The fit by a power law is very good (correlation  $> 0.7$ ) for  $\ln(kR) < 1.5$ , but worse (i.e., data are more noisy) for larger values of  $\ln(kR)$ . Noise may be the reason why  $S(kR)$  stays clamped at 0.3 for  $2 < \ln(kR) < 3$  and does not decrease to zero.

A basic difference between stable blast waves in nitrogen and unstable blast waves in xenon is that the former propagate in a gas with adiabatic index  $\gamma_N = 1.3 \pm 0.1$ , and the latter in a gas with  $\gamma_{Xe} = 1.06 \pm 0.02$ . To derive  $\gamma_{Xe}$  we utilize the observation that blast waves in nitro-

gen and xenon propagate according to the Taylor-Sedov blast-wave relation<sup>10</sup>

$$d \propto \left[ \frac{75(\gamma-1)(\gamma+1)^2}{16\pi(3\gamma-1)\rho_0} \right]^{1/5} t^{2/5},$$

where  $d$  is the distance between the focal spot and the blast-wave front and  $\rho_0$  is the gas mass density. Therefore, by dividing the measured  $d$  in nitrogen by the measured  $d$  in xenon at any given time we arrive at a relationship between  $\gamma_{Xe}$ ,  $\gamma_N$ , and the mass of each gas species. Solving numerically for  $\gamma_{Xe}$  as a function of  $\gamma_N$ , we find that as  $\gamma_N$  varies from 1 to  $\frac{5}{3}$ ,  $\gamma_{Xe}$  varies from 1 to 1.13. Hence, for any reasonable value of  $\gamma_N$  the value of  $\gamma_{Xe}$  is less than 1.13. In past experiments<sup>8</sup> we have measured  $\gamma_N$  to be  $1.3 \pm 0.1$ , which implies that  $\gamma_{Xe} = 1.06 \pm 0.02$ .

$\gamma_{Xe}$  is lower than  $\gamma_N$  because prior to the arrival of the blast wave xenon gas radiates much more than nitrogen gas. (Radiation increases the degrees of freedom within a gas and hence reduces its effective  $\gamma$ .) This is demonstrated by examining the spectrum of light emanating from a spot in front of the laser's focal point [Fig. 3(d)]. In nitrogen gas the laser-induced explosion produces little measurable emission prior to the arrival of the blast wave. Immediately before the blast wave arrives at the observation point there is a slight increase of  $N^{1+}$  and  $N^{2+}$  lines: These lines are probably excited by UV or heat from the blast wave. When the blast front arrives, there is a sudden increase in emission from the  $N^{1+}$ ,  $N^{2+}$ , and target  $C^{2+}$  lines, as well as an increase in continuum emission. In contrast, xenon emits copiously in many  $Xe^{1+}$  and some  $Xe^{2+}$  lines from the moment the laser strikes the foil. Arrival of the unstable blast wave is signaled by a more gradual increase in continuum emission, but line emission is not changed significantly. We conclude, therefore, that it is the radiation in xenon

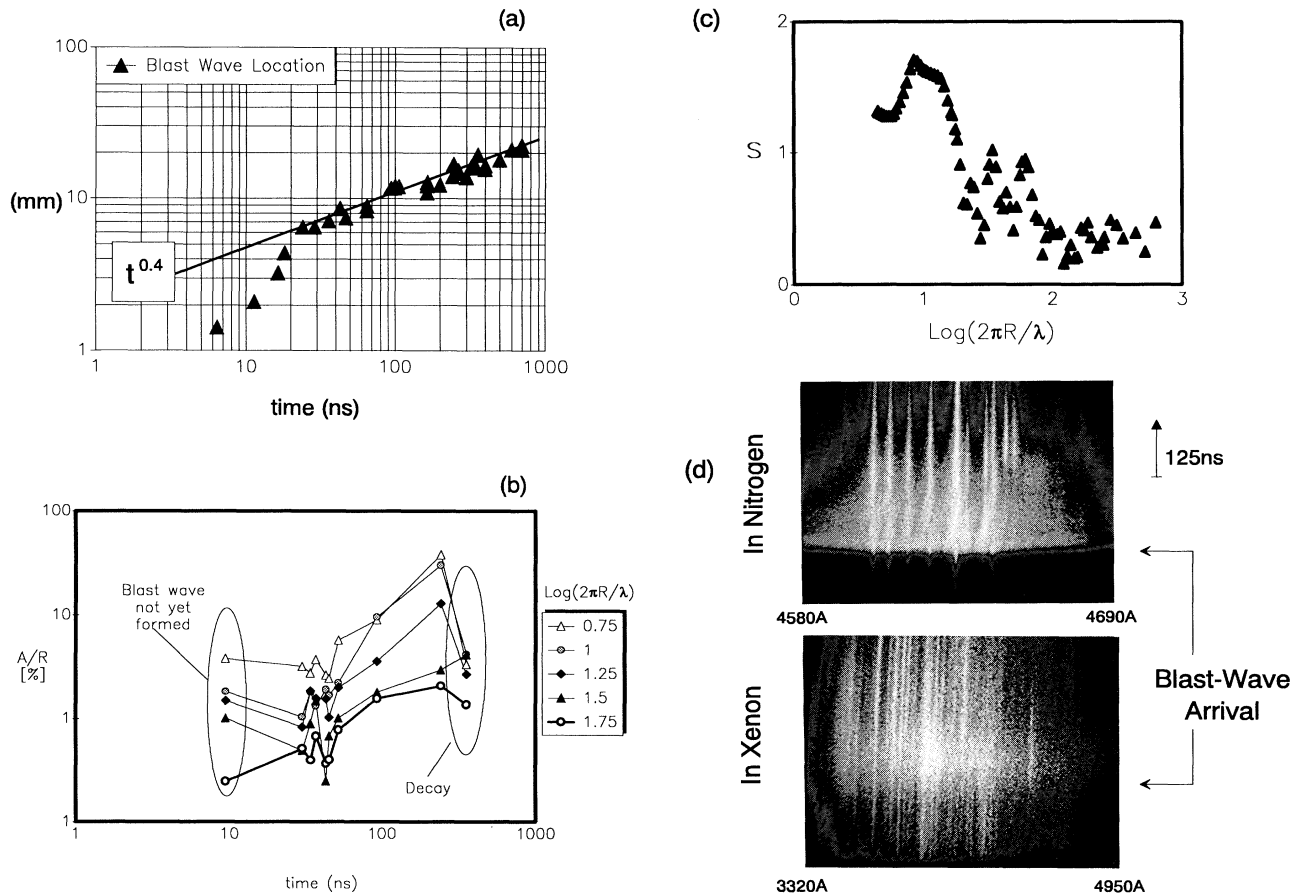


FIG. 3. Instability growth. (a) Blast-wave trajectory. (b) Amplitude growth as a function of time for different values of  $\ln(kR)$ . The scatter of points between 30 and 45 ns at each value of  $\ln(kR)$  indicates the shot-to-shot reproducibility in this experiment. (c) Growth exponent  $S(kR)$ . (d) Emission spectra as a function of time in nitrogen and xenon gas from a spot which is 2 cm from the laser's focal point.

which reduces its effective  $\gamma$  below that of nitrogen. Among the various theories,<sup>2-4</sup> the one by Vishniac and Ryu<sup>4</sup> predicts that Taylor-Sedov blast waves in a uniform gas with  $\gamma < 1.2$  will become unstable. In spherical geometry, perturbations are predicted to grow as  $Y_{lm}(\theta, \phi)t^{S(l)}$ , where  $Y_{lm}$  are spherical harmonic modes. In planar geometry, perturbations grow as  $e^{iky}t^{S(kx)}$ , where  $x$  is the direction of blast propagation. For  $\gamma = 1.1$ , numerically calculated maximum growth occurs at  $\ln(l) \approx 1.5$  with  $\text{Re}[S(l)] \approx 0.5$ , and  $\ln(kx) \approx 1.2$  with  $\text{Re}[S(kx)] \approx 0.3$ , for the spherical and planar cases, respectively. For  $\gamma = 1.06$ , a less precise but analytic calculation<sup>11</sup> in spherical geometry gives maximum growth at  $\ln(l) \approx 1.7$ , with  $\text{Re}[S(l)] \approx 0.7$ . Theory does not treat the large-amplitude regime where saturation or stabilization may occur.

The basic predictions of this theory agree with our observations of  $t^S$  growth in a low- $\gamma$  uniform gas, but there are differences in the details. For  $\gamma = 1.06$  we measure

maximum growth at  $\ln(kR) \approx 1$  with  $S \approx 1.6$ , whereas theory predicts maximum growth at higher  $\ln(l)$  and lower  $S$ : Theory predicts virtually no growth ( $S \approx 0.04$ ) at  $\ln(l) = 1$ . Possible stabilization is seen at 400 ns. We remind the reader, however, that the wave numbers in our experiment were obtained from the projection onto a plane of the edge of an unstable sphere. Thus,  $kR$  is not identical to either  $l$  or  $kx$ . Also, there are a few alternative explanations for the observed apparent stabilization. One may argue, for example, that the stabilization is a real nonlinear phenomenon; or that  $\gamma$  is large at some point far from the focal spot and the blast wave stabilized because it moved into that region; or that the instability is still growing but the density gradients in the spikes are too gentle to measure at late times. These issues will be addressed in future work.

We point out that the phenomenon described here is not the Rayleigh-Taylor instability commonly associated with decelerating systems. That instability is caused by

opposing density and pressure gradients and exhibits exponential growth. This instability is associated with the sloshing of material within the blast-wave shell and exhibits power-law growth. Our instability mechanism may be briefly explained as follows:<sup>4</sup> The thermal pressure which drives the blast wave is perpendicular to the local blast shell surface, while the external ram pressure (ambient density times square of blast speed) is antiparallel to the direction of propagation. In a uniform blast wave the front and the direction of propagation are orthogonal so that the thermal and ram pressures are both perpendicular to the shell surface. But in a rippled blast wave the thermal pressure is no longer parallel to the propagation direction while the ram-pressure orientation does not change. Therefore, there appears a net pressure along the blast front surface that accelerates mass into the lagging trough parts of the ripple. The now heavier trough has more momentum, slows less, and consequently moves ahead. Then the process reverses and an oscillation ensues. This oscillation is damped out at wavelengths comparable to the blast shell radius and wavelengths much larger than the shell thickness. Otherwise, it grows. Since shell thickness is related to  $\gamma$ , so is the growth exponent of the instability.

In conclusion, we have shown experimentally, for the first time, that Taylor-Sedov blast waves in a uniform gas are unstable when the adiabatic index  $\gamma$  is sufficiently low, in our case 1.06. Perturbed amplitudes grow as a power of time. Our results confirm the basic predictions of Vishniac and Ryu.

We are grateful to Levi Daniels, Jim Ford, and Nicholas Nocerino for their expert and dedicated technical assistance. We acknowledge electronic-mail exchanges with Dr. Ethan Vishniac on the utilization of the analytic theory in Ref. 4. The authors also thank Dr. Jim Barthel and Dr. David Book for reviewing early versions of this manuscript. This work is supported by the Office of Naval Research and the Defense Nuclear Agency.

<sup>(a)</sup>Present address: Laser-Plasma Branch, Plasma Physics Division, Washington, DC 20375-5000.

<sup>(b)</sup>Present address: Science Applications International, McLean, VA 22101.

<sup>(c)</sup>Present address: Physical Sciences, Inc., Alexander, VA 23701.

<sup>(d)</sup>Present address: Physics Department, SW Texas State University, San Marcos, TX 78666.

<sup>1</sup>Sample works: R. A. Chevalier, *Astrophys. J.* **207**, 872 (1976); H. Gerola and P. E. Seiden, *Astrophys. J.* **223**, 129 (1978); J. P. Ostriker and L. L. Cowie, *Astrophys. J. Lett.* **243**, L127 (1981); V. Trimble, *Rev. Mod. Phys.* **60**, 859 (1988).

<sup>2</sup>P. A. Isenberg, *Astrophys. J.* **217**, 597 (1977); A. Cheng, *Astrophys. J.* **227**, 955 (1979); I. B. Bernstein and D. L. Book, *Astrophys. J.* **240**, 223 (1980); B. Gaffet, *Astrophys. J.* **279**, 419 (1984); B. Gaffet, *Astron. Astrophys.* **135**, 94 (1984); I. Kohlberg, Kohlberg Associates Report No. KAINRL02-89, 1989 (unpublished).

<sup>3</sup>W. I. Newman, *Astrophys. J.* **236**, 880 (1980).

<sup>4</sup>E. T. Vishniac, *Astrophys. J.* **274**, 152 (1983); D. Ryu and E. T. Vishniac, *Astrophys. J.* **313**, 820 (1987); E. T. Vishniac and D. Ryu, *Astrophys. J.* **337**, 917 (1989).

<sup>5</sup>L. I. Sedov, *Similarity and Dimensional Methods in Mechanics* (Academic, New York, 1959).

<sup>6</sup>P. G. Burkhalter *et al.*, *Phys. Fluids* **26**, 3650 (1983).

<sup>7</sup>J. Grun *et al.*, *Appl. Phys. Lett.* **39**, 545 (1981); *Phys. Fluids* **26**, 588 (1983); **29**, 3390 (1986).

<sup>8</sup>B. H. Ripin *et al.*, in *Laser Interactions and Related Plasma Phenomena*, edited by H. Hora and G. H. Miley (Plenum, New York, 1986), Vol. 7, pp. 857-877; J. Grun *et al.*, *ibid.* (to be published), Vol. 9; and (to be published).

<sup>9</sup>An 80% cosine taper (Tukey) window is used to eliminate mismatches at the ends of the region to be transformed.

<sup>10</sup>Ya. B. Zel'dovich and Yu. P. Raizer, *Physics of Shock Waves and High-Temperature Hydrodynamic Phenomena* (Academic, New York, 1966); the claim that  $\gamma_{Xe} < 1.13$  for any reasonable value of  $\gamma_N$  relies primarily on the accuracy of the Chernyi blast-wave solution on page 99. Error bars in  $\gamma_{Xe}$  result from the error bars in  $\gamma_N$ .

<sup>11</sup>Calculated using equation 19 in the 1989 paper of Ref. 4. In that paper we used  $D = (\gamma - 1)/3(\gamma + 1)(1 - \beta)$ .

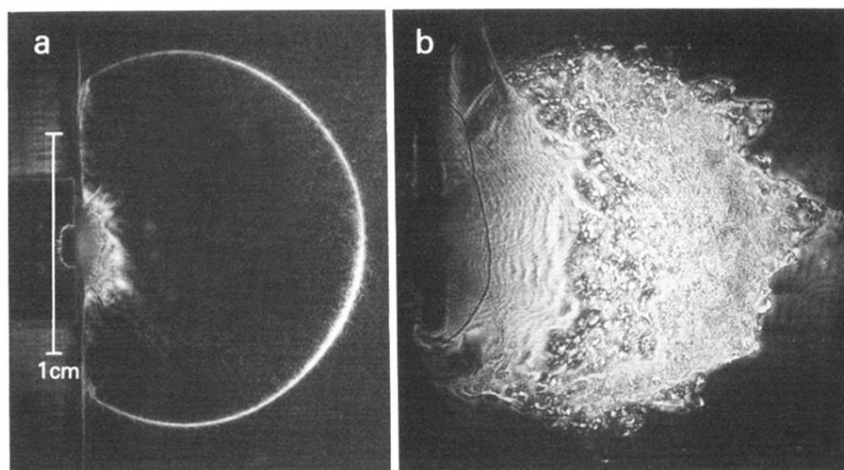


FIG. 2. Dark-field shadowgraph of (a) a stable blast wave in nitrogen gas, and (b) an unstable blast wave in xenon gas (at 243 ns).

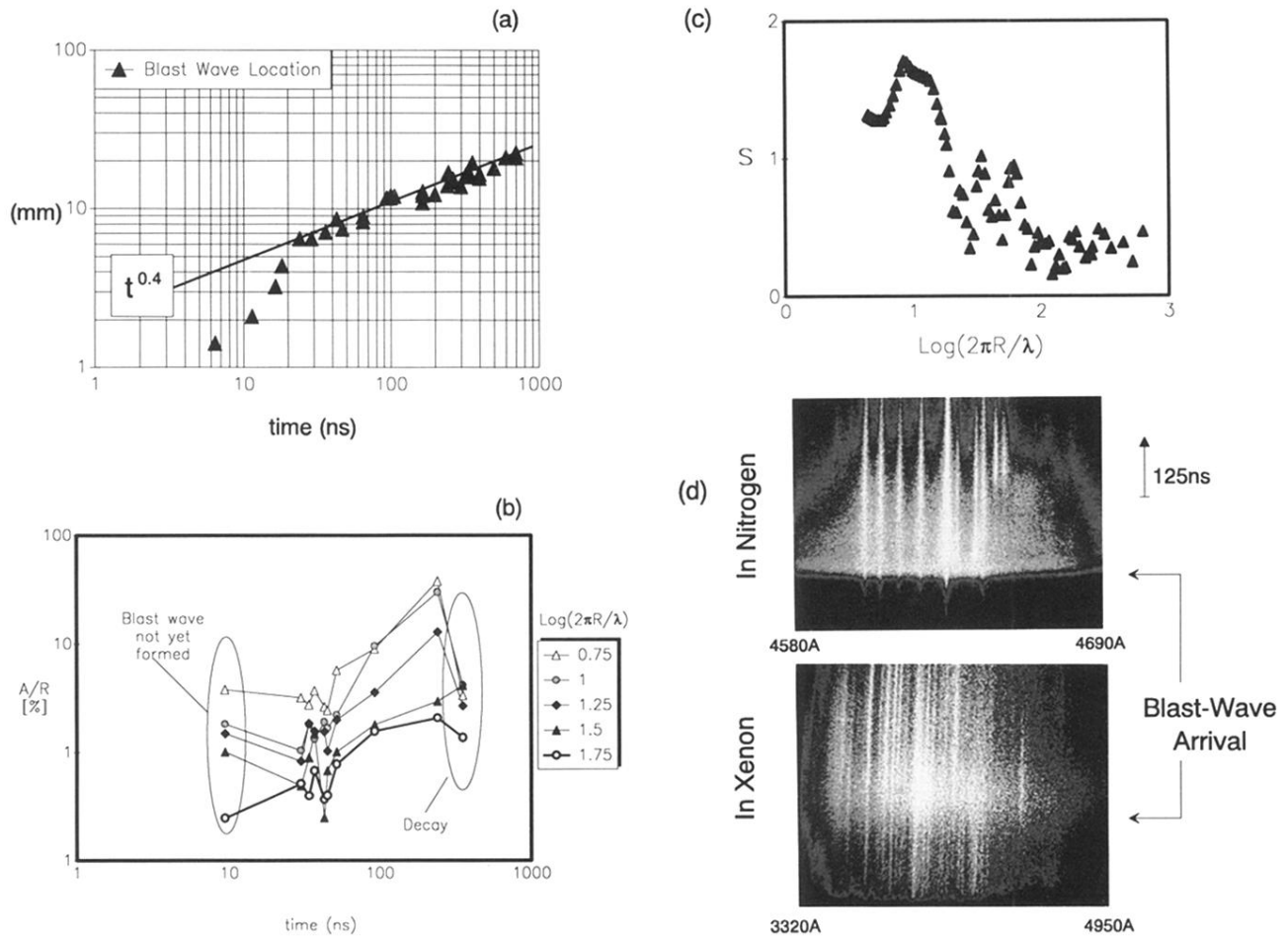


FIG. 3. Instability growth. (a) Blast-wave trajectory. (b) Amplitude growth as a function of time for different values of  $\ln(kR)$ . The scatter of points between 30 and 45 ns at each value of  $\ln(kR)$  indicates the shot-to-shot reproducibility in this experiment. (c) Growth exponent  $S(kR)$ . (d) Emission spectra as a function of time in nitrogen and xenon gas from a spot which is 2 cm from the laser's focal point.